ECE414/514
Electronics Packaging
Spring 2012 Lecture 13
Materials A:
Properties, Metals, Solder, Ceramics

James E. Morris
Dept of Electrical & Computer Engineering
Portland State University

Lecture Topics

- Material properties
- Metals
  - Wirebond
  - Leadframe
    - Adhesion
  - Solder
    - Diffusion
  - Die attach
- Ceramics
  - LTCC
- FR4 (epoxy/glass laminate)

Mechanical Properties

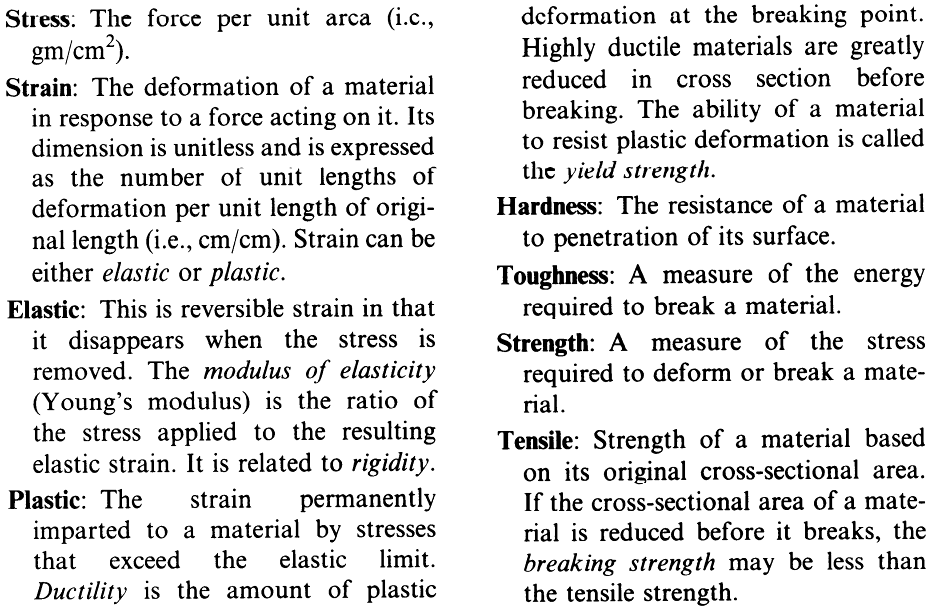

Stress: The force per unit area (i.e., gm/cm^2).

Strain: The deformation of a material in response to a force acting on it. Its dimension is unitless and is expressed as the number of unit lengths of deformation per unit length of original length (i.e., cm/cm). Strain can be either *elastic* or *plastic*.

Elastic: This is reversible strain in that it disappears when the stress is removed. The *modulus of elasticity* (Young's modulus) is the ratio of the stress applied to the resulting elastic strain. It is related to *rigidity*.

Plastic: The strain permanently imparted to a material by stresses that exceed the elastic limit. *Ductility* is the amount of plastic deformation at the breaking point. Highly ductile materials are greatly reduced in cross section before breaking. The ability of a material to resist plastic deformation is called the *yield strength*.

Hardness: The resistance of a material to penetration of its surface.

Toughness: A measure of the energy required to break a material.

Strength: A measure of the stress required to deform or break a material.

Tensile: Strength of a material based on its original cross-sectional area. If the cross-sectional area of a material is reduced before it breaks, the *breaking strength* may be less than the tensile strength.

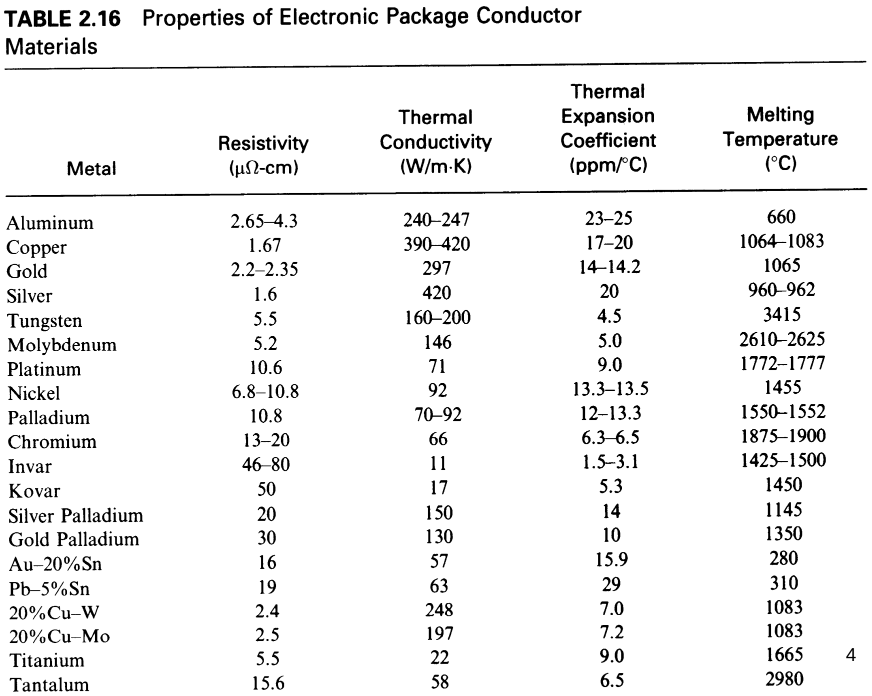

TABLE 2.16 Properties of Electronic Package Conductor Materials

Metal	Resistivity (μΩ-cm)	Thermal Conductivity (W/m·K)	Thermal Expansion Coefficient (ppm/°C)	Melting Temperature (°C)
Aluminum	2.65–4.3	240–247	23–25	660
Copper	1.67	390–420	17–20	1064–1083
Gold	2.2–2.35	297	14–14.2	1065
Silver	1.6	420	20	960–962
Tungsten	5.5	160–200	4.5	3415
Molybdenum	5.2	146	5.0	2610–2625
Platinum	10.6	71	9.0	1772–1777
Nickel	6.8–10.8	92	13.3–13.5	1455
Palladium	10.8	70–92	12–13.3	1550–1552
Chromium	13–20	66	6.3–6.5	1875–1900
Invar	46–80	11	1.5–3.1	1425–1500
Kovar	50	17	5.3	1450
Silver Palladium	20	150	14	1145
Gold Palladium	30	130	10	1350
Au–20%Sn	16	57	15.9	280
Pb–5%Sn	19	63	29	310
20%Cu–W	2.4	248	7.0	1083
20%Cu–Mo	2.5	197	7.2	1083
Titanium	5.5	22	9.0	1665
Tantalum	15.6	58	6.5	2980

Metal (bond wire) and Molding Materials

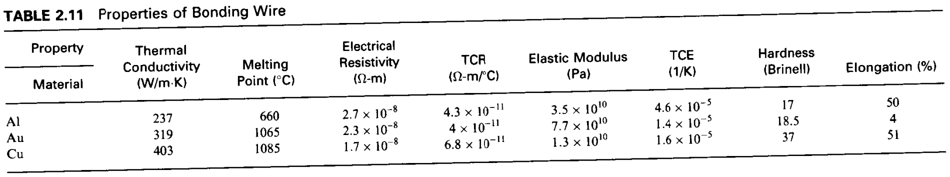

TABLE 2.11 Properties of Bonding Wire

Property / Material	Thermal Conductivity (W/m·K)	Melting Point (°C)	Electrical Resistivity (Ω-m)	TCR (Ω-m/°C)	Elastic Modulus (Pa)	TCE (1/K)	Hardness (Brinell)	Elongation (%)
Al	237	660	2.7×10^{-8}	4.3×10^{-11}	3.5×10^{10}	4.6×10^{-5}	17	50
Au	319	1065	2.3×10^{-8}	4×10^{-11}	7.7×10^{10}	1.4×10^{-5}	18.5	4
Cu	403	1085	1.7×10^{-8}	6.8×10^{-11}	1.3×10^{10}	1.6×10^{-5}	37	51

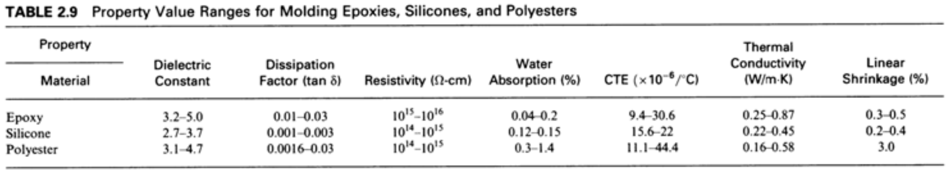

TABLE 2.9 Property Value Ranges for Molding Epoxies, Silicones, and Polyesters

Property / Material	Dielectric Constant	Dissipation Factor (tan δ)	Resistivity (Ω-cm)	Water Absorption (%)	CTE (×10^{-6}/°C)	Thermal Conductivity (W/m·K)	Linear Shrinkage (%)
Epoxy	3.2–5.0	0.01–0.03	10^{15}–10^{16}	0.04–0.2	9.4–30.6	0.25–0.87	0.3–0.5
Silicone	2.7–3.7	0.001–0.003	10^{14}–10^{15}	0.12–0.15	15.6–22	0.22–0.45	0.2–0.4
Polyester	3.1–4.7	0.0016–0.03	10^{14}–10^{15}	0.3–1.4	11.1–44.4	0.16–0.58	3.0

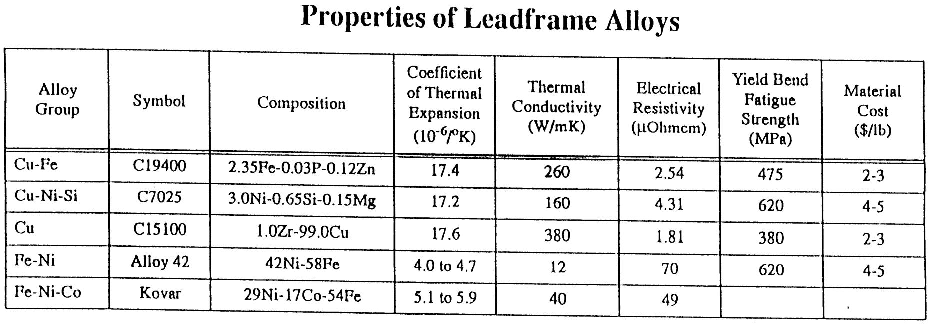

Properties of Leadframe Alloys

Alloy Group	Symbol	Composition	Coefficient of Thermal Expansion (10^{-6}/°K)	Thermal Conductivity (W/mK)	Electrical Resistivity (μOhmcm)	Yield Bend Fatigue Strength (MPa)	Material Cost ($/lb)
Cu-Fe	C19400	2.35Fe-0.03P-0.12Zn	17.4	260	2.54	475	2-3
Cu-Ni-Si	C7025	3.0Ni-0.65Si-0.15Mg	17.2	160	4.31	620	4-5
Cu	C15100	1.0Zr-99.0Cu	17.6	380	1.81	380	2-3
Fe-Ni	Alloy 42	42Ni-58Fe	4.0 to 4.7	12	70	620	4-5
Fe-Ni-Co	Kovar	29Ni-17Co-54Fe	5.1 to 5.9	40	49		

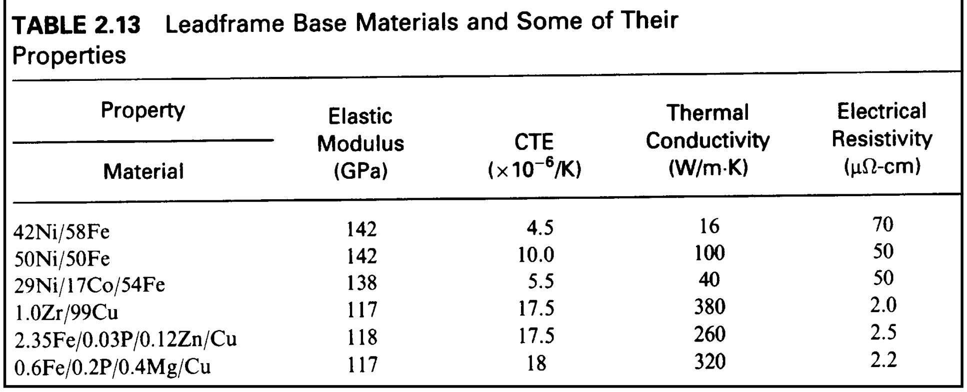

TABLE 2.13 Leadframe Base Materials and Some of Their Properties

Property / Material	Elastic Modulus (GPa)	CTE (×10^{-6}/K)	Thermal Conductivity (W/m·K)	Electrical Resistivity (μΩ-cm)
42Ni/58Fe	142	4.5	16	70
50Ni/50Fe	142	10.0	100	50
29Ni/17Co/54Fe	138	5.5	40	50
1.0Zr/99Cu	117	17.5	380	2.0
2.35Fe/0.03P/0.12Zn/Cu	118	17.5	260	2.5
0.6Fe/0.2P/0.4Mg/Cu	117	18	320	2.2

Adhesion

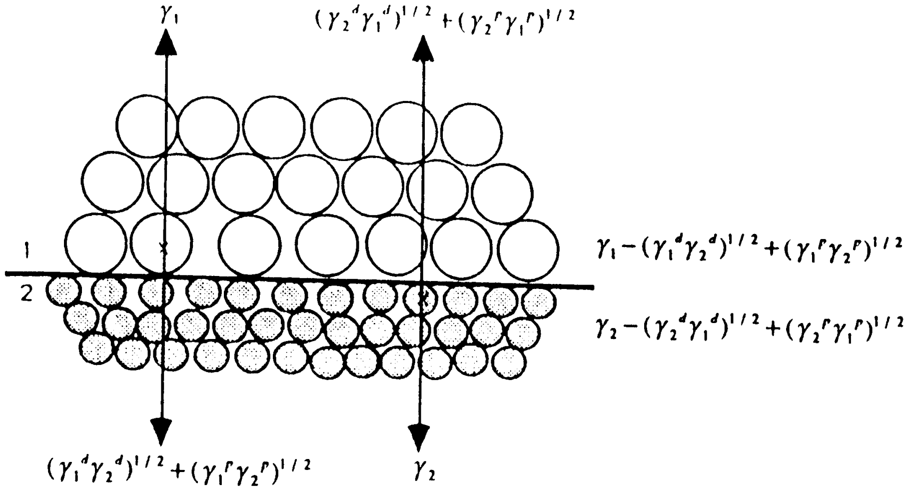

Figure 2.1 **A simple interface model.**

Consider 2 materials as shown, with

surface tensions (cohesive forces) γ_1 and γ_2

and interfacial tension γ_{12}.

Then the work of adhesion $W_a = \gamma_1 + \gamma_2 - \gamma_{12}$

Consider molecule X in the surface layer of top material 1.
It is attracted upwards by force γ_1 and down by force γ_{12}
γ_{12} is made up of:

dispersion forces γ^d ,

(due to polarization of the molecule below,) and

polar forces γ^p

(due to dipole interactions.)

$$\gamma_{12} = \gamma_1 + \gamma_2 - 2[(\gamma_1^d \gamma_2^d)^{1/2} + (\gamma_1^p \gamma_2^p)^{1/2}]$$

$$W_a = 2[(\gamma_1^d \gamma_2^d)^{1/2} + (\gamma_1^p \gamma_2^p)^{1/2}]$$

Contact Angle:

$$\gamma_{12} = \gamma_2 - \gamma_1 \cos\theta$$

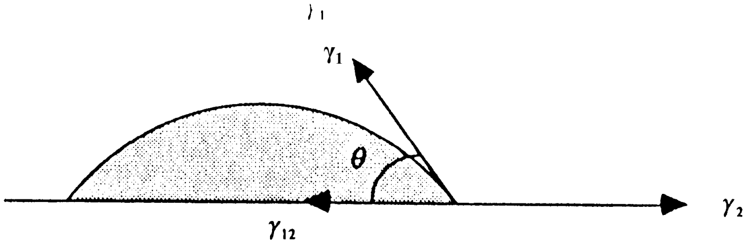

$$\gamma_{12} = \gamma_2 - \gamma_1 \cos\theta$$

Figure 2.2 **The relationship between the interfacial energy and contact angle by a liquid of known surface tension.**

Typically

$$\gamma^p \ll \gamma^d \text{, and } \gamma_{Cu}{}^d \sim \gamma_{MC}{}^d \text{, so } \mathbf{W_a} \sim 2\gamma^d$$

Mold Compound	Contact Angle, H_2O	Contact Angle, CH_2I_2	γ^d, dyne/cm	γ^p, dyne/cm	W_a, erg/cm^2
Cu-110	95.4	51.4	36.4	0.85	—
MC-100	91	52	31.3	2.2	70.2
MC-101	95	57	35.5	1.6	74.2
MC-102	90	44	36.6	1.3	75.1
MC-103	83	49	38.9	5.0	79.4
MC-104	96	51	40.3	0.79	78.2

Table 2.1 **Measured values of contact angles and calculated values of γ^d, γ^p, and W_a.**

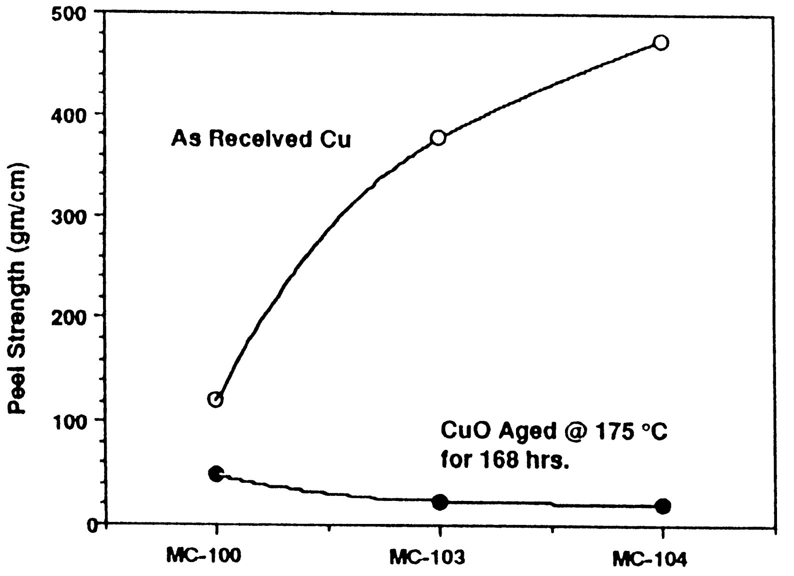

Figure 2.6 Effect of copper oxide structures on peel adhesion.

Oxidation: γ^p increases (polarization effects)

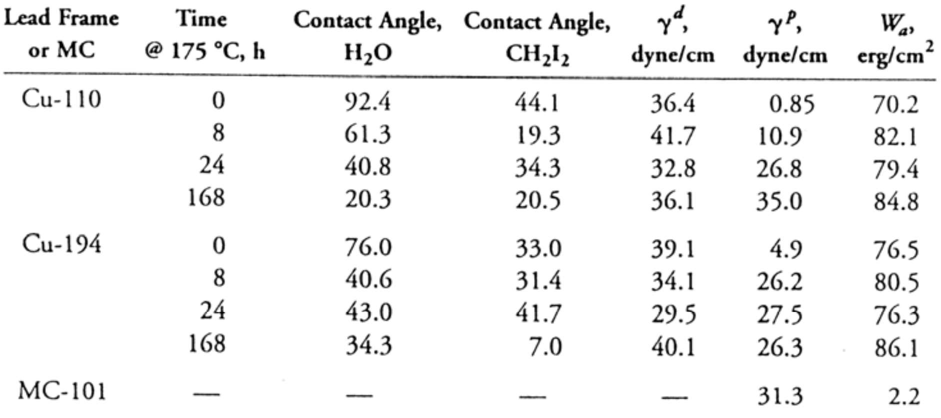

Lead Frame or MC	Time @ 175 °C, h	Contact Angle, H_2O	Contact Angle, CH_2I_2	γ^d, dyne/cm	γ^p, dyne/cm	W_a, erg/cm^2
Cu-110	0	92.4	44.1	36.4	0.85	70.2
	8	61.3	19.3	41.7	10.9	82.1
	24	40.8	34.3	32.8	26.8	79.4
	168	20.3	20.5	36.1	35.0	84.8
Cu-194	0	76.0	33.0	39.1	4.9	76.5
	8	40.6	31.4	34.1	26.2	80.5
	24	43.0	41.7	29.5	27.5	76.3
	168	34.3	7.0	40.1	26.3	86.1
MC-101	—	—	—	—	31.3	2.2

Table 2.2 Cu lead frame surface energy changes accompanying thermal oxidation.

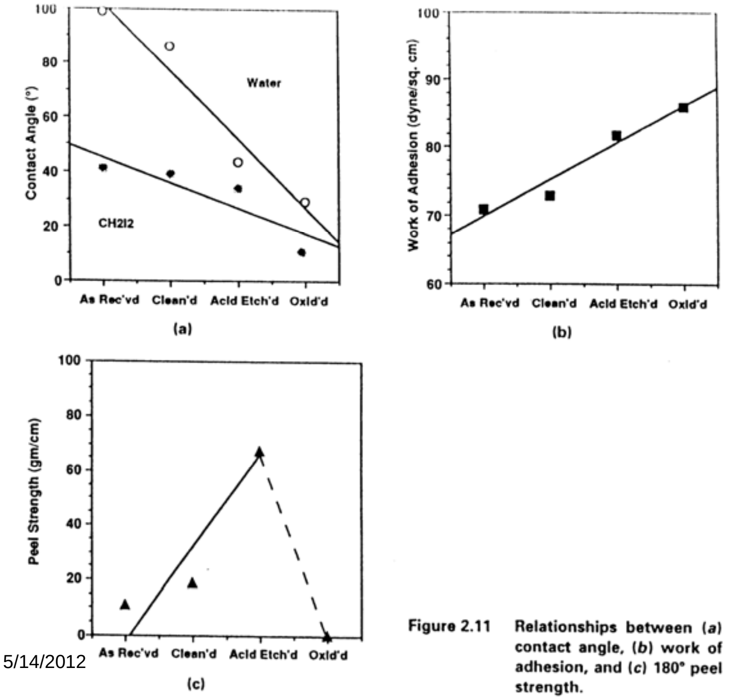

Figure 2.11 Relationships between (*a*) contact angle, (*b*) work of adhesion, and (*c*) 180° peel strength.

$$W_a = 2[(\gamma_1^d \gamma_2^d)^{1/2} + (\gamma_1^p \gamma_2^p)^{1/2}]$$

Lead Frame or MC	γ^d, dyne/cm	γ^p, dyne/cm	Work of Adhesion, erg/cm^2 MC-300/ Lead Frame	MC-301/ Lead Frame	MC-302/ Lead Frame
Cu-110	36.4	0.85	70.2	72.7	73.0
Alloy-42	31.1	0.66	64.8	67.0	67.3
Cu/Ni	29.2	0.33	62.2	63.8	64.0
MC-300	31.3	2.2	—	—	—
MC-301	31.5	7.3	—	—	—
MC-302	31.8	7.3	—	—	—

Table 2.3 Polar and dispersion character of various lead frames and their work of adhesion with typical mold compounds.

Solder

- Phase diagrams
- Lever Rule
- Eutectic solder

- Diffusion

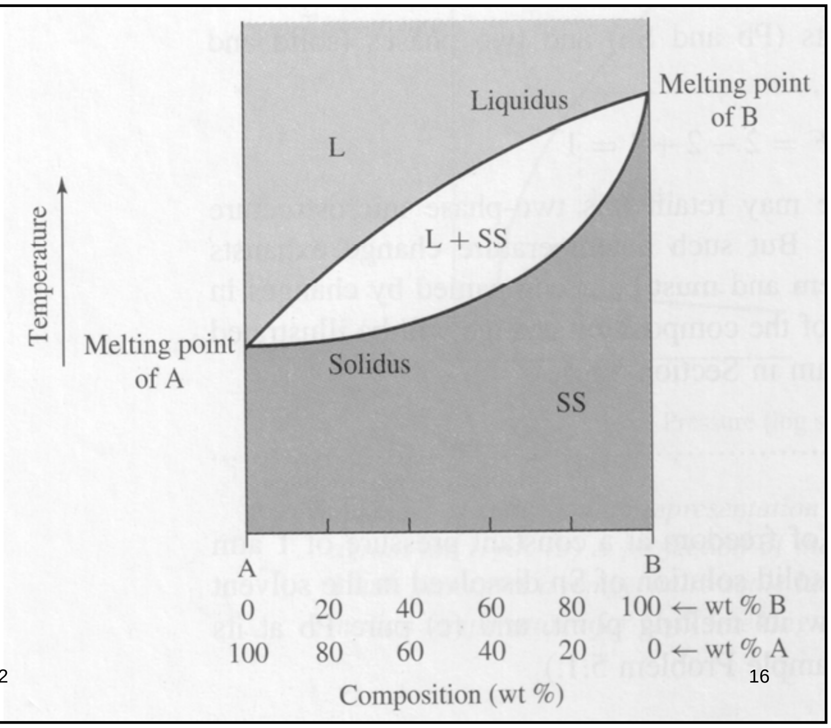

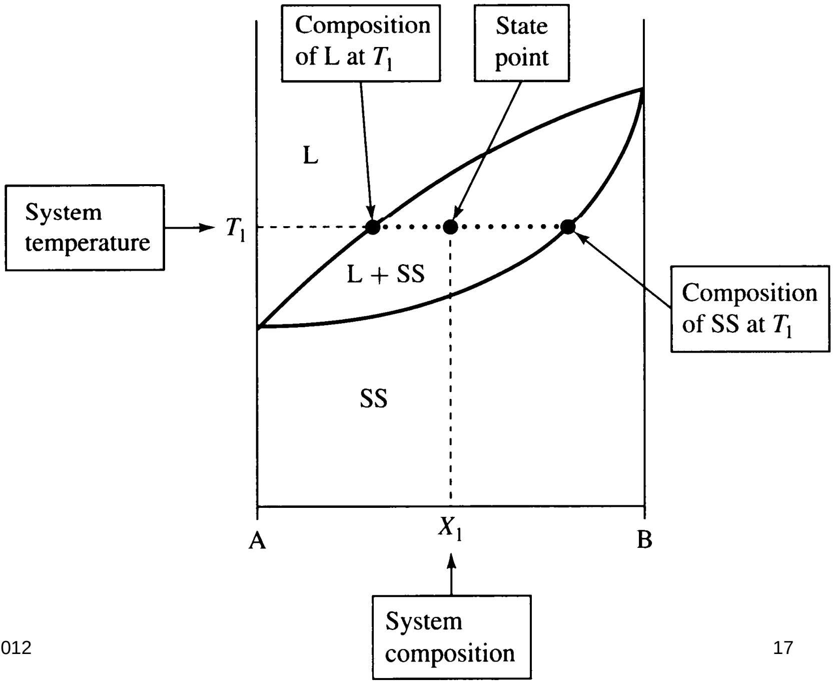

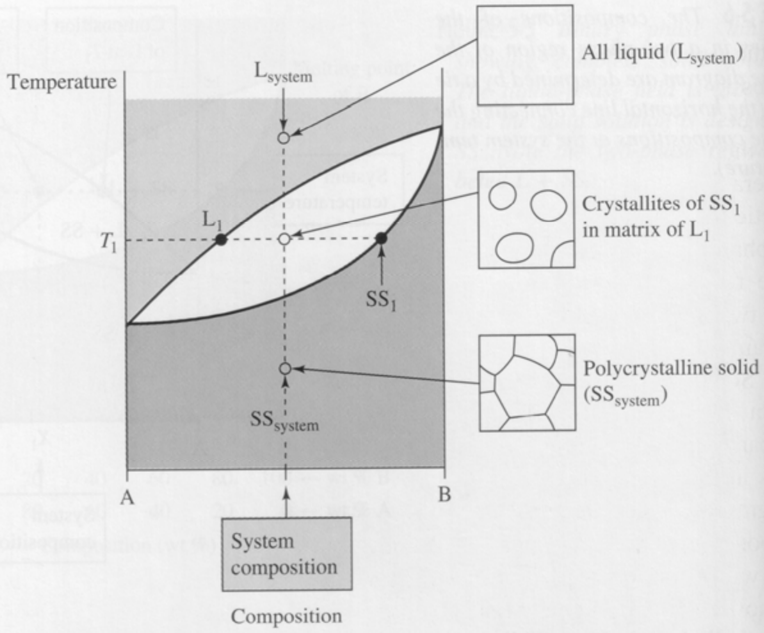

FIGURE 5-8 *Various microstructures characteristic of different regions in the complete solid-solution phase diagram.*

Proportions and compositions of liquid and solid solution

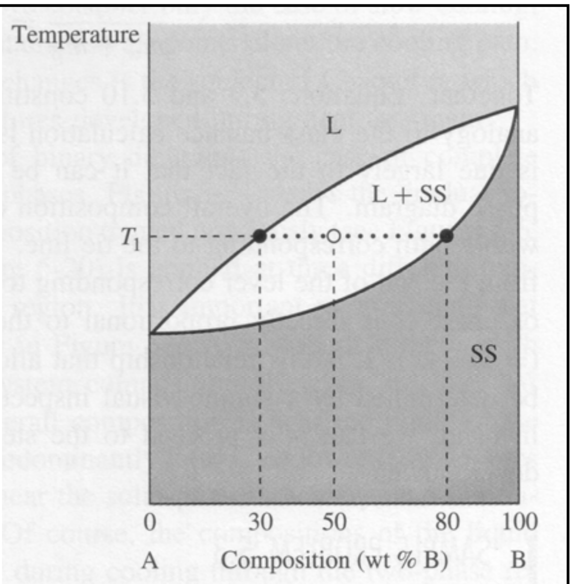

$$m_L + m_{SS} = m_{total}$$
$$0.30m_L + 0.80m_{SS} = 0.50m_{total}$$
$$\rightarrow m_L = 0.60m_{total}$$
$$m_{SS} = 0.40m_{total}$$

Lever Rule

$$\mathbf{M_l / M_{tot}} = s / (s + l)$$

$$\mathbf{M_s / M_{tot}} = l / (s + l)$$

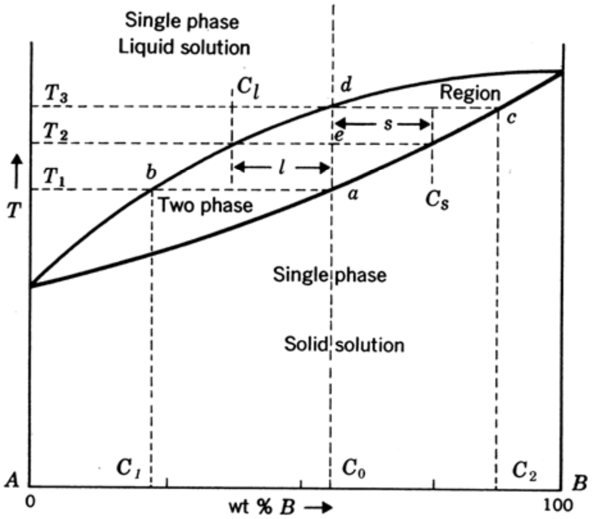

Figure 5-3 **Hypothetical liquid-solid region of a phase diagram.**

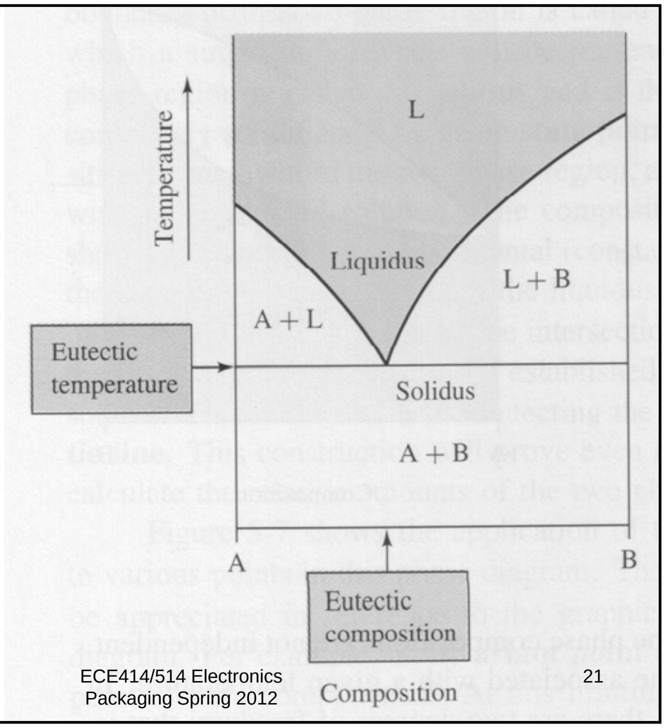

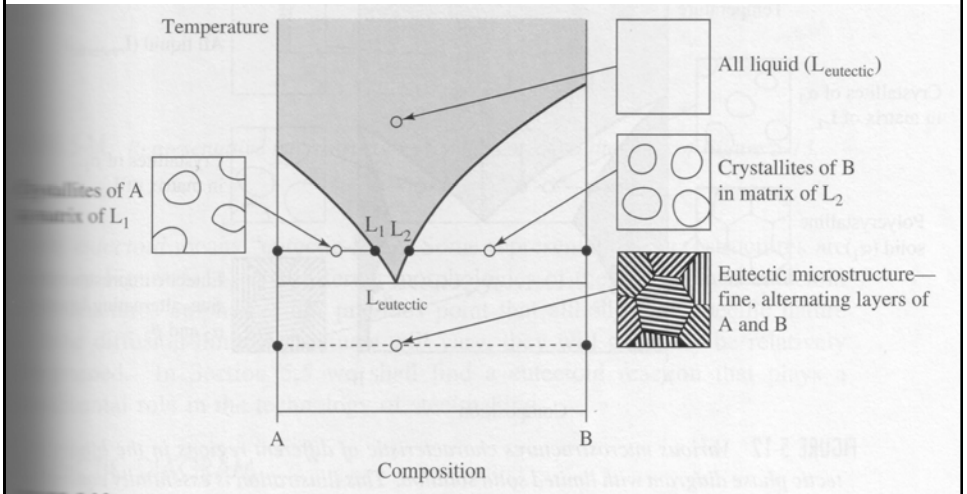

5-10 Various microstructures characteristic of different regions in a binary eutec-
phase diagram with no solid solution.

Solid solutions

α phase of A

β phase of B

Crystallite mixture

α + β

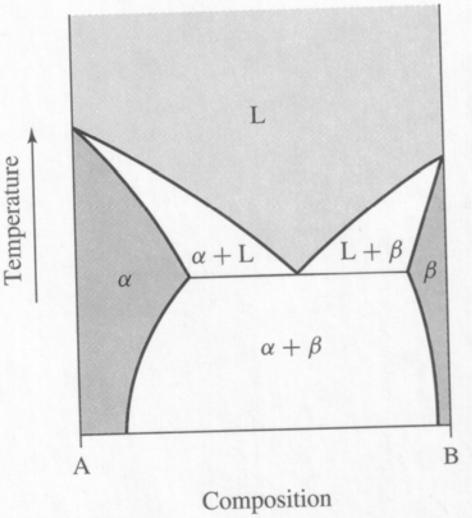

FIGURE 5-11 *Binary eutectic phase diagram with limited solid solution. The only difference from Figure 5-9 is the presence of solid-solution regions α and β.*

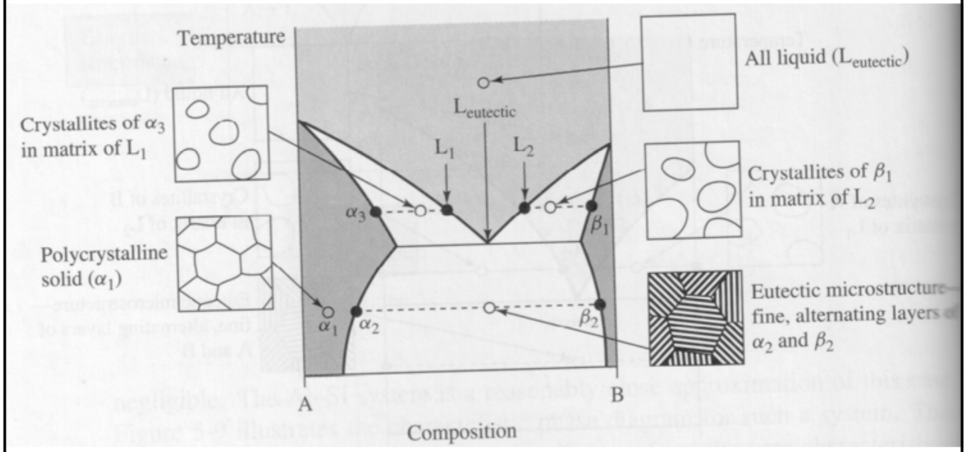

Sn – Pb Phase Diagram

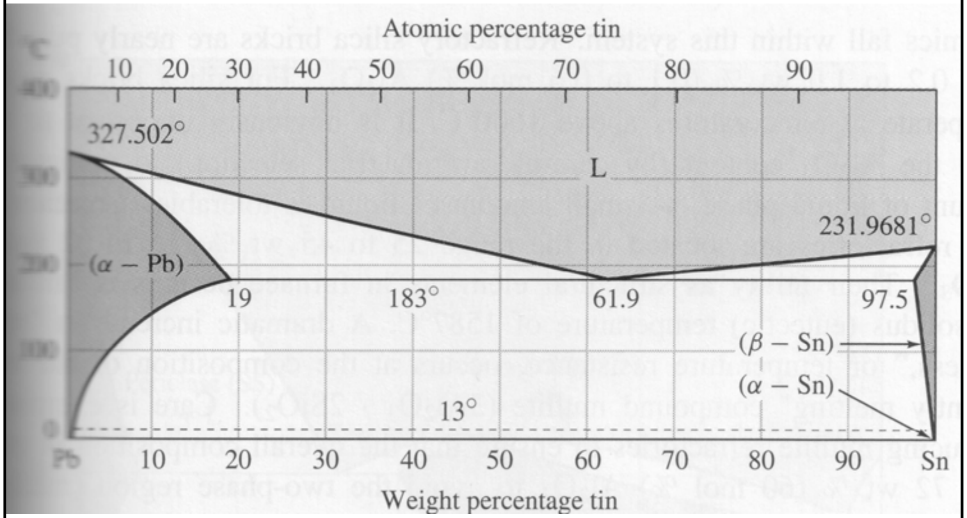

Note: Atomic % vs Weight %

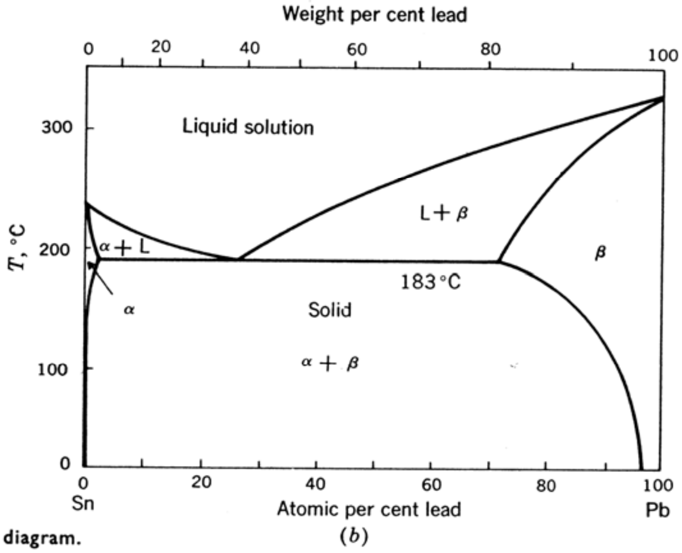

Figure 5-7 (b) **Sn-Pb phase diagram.**

Cooling

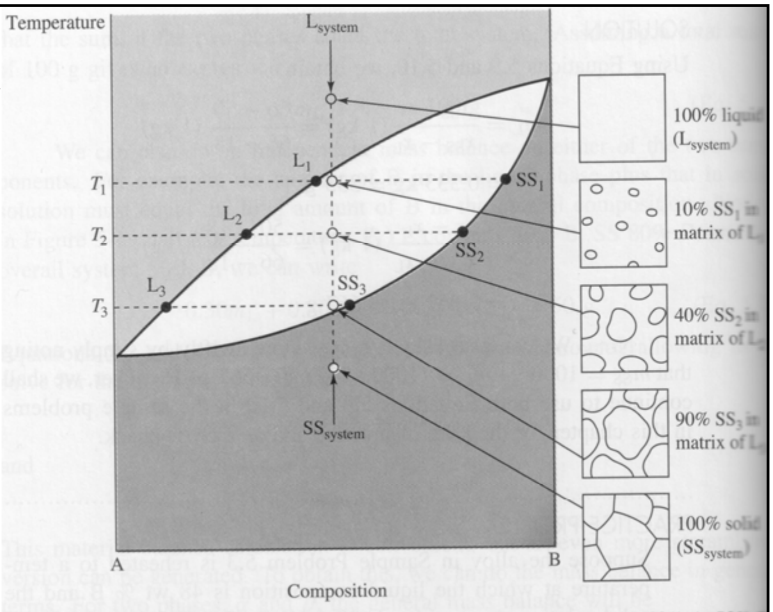

FIGURE 5-21 *Microstructural development during the slow cooling of a 50% A–50% composition in a phase diagram with complete solid solution. At each temperature the amounts of the phases in the microstructure correspond to a lever rule calculation. The microstructure at T_2 corresponds to the calculation in Figure 5-19.*

5/14/2012

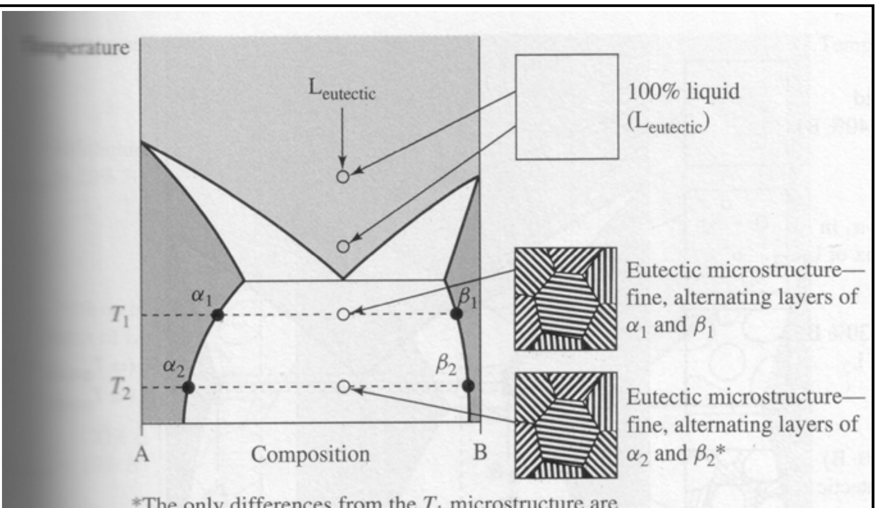

*The only differences from the T_1 microstructure are the phase compositions and the relative amounts of each phase. For example, the amount of β will be proportional to:

$$\frac{x_{eutectic} - x_\alpha}{x_\beta - x_\alpha}$$

Eutectic Cooling

URE 5-22 *Microstructural development during the slow cooling of a eutectic composition.*

Off-eutectic composition

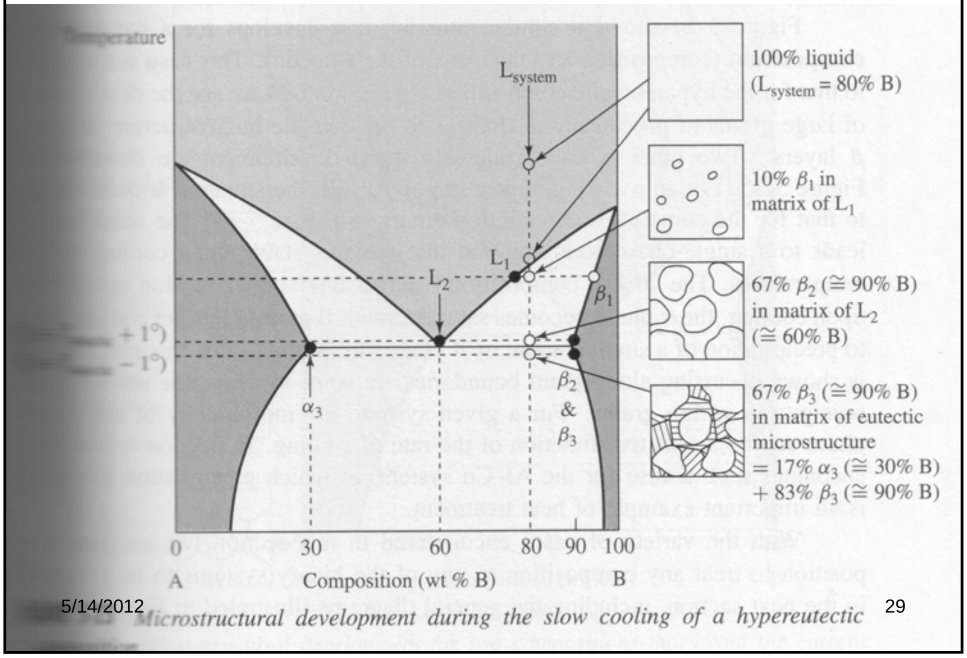

Microstructural development during the slow cooling of a hypereutectic

Intermetallic Diffusion
Brittle IMCs (alloys)

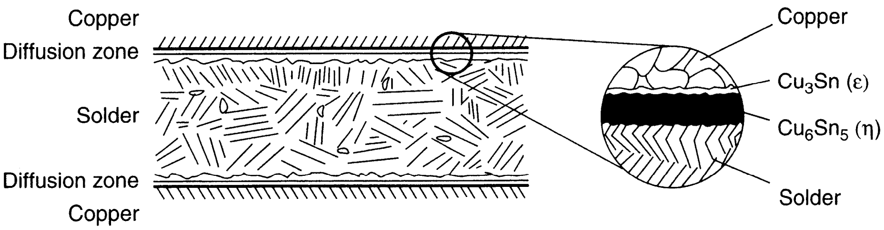

FIGURE 5.17 Cross-section through a soldered joint, made with eutectic solders.

Purple Plague ($AuAl_2$)

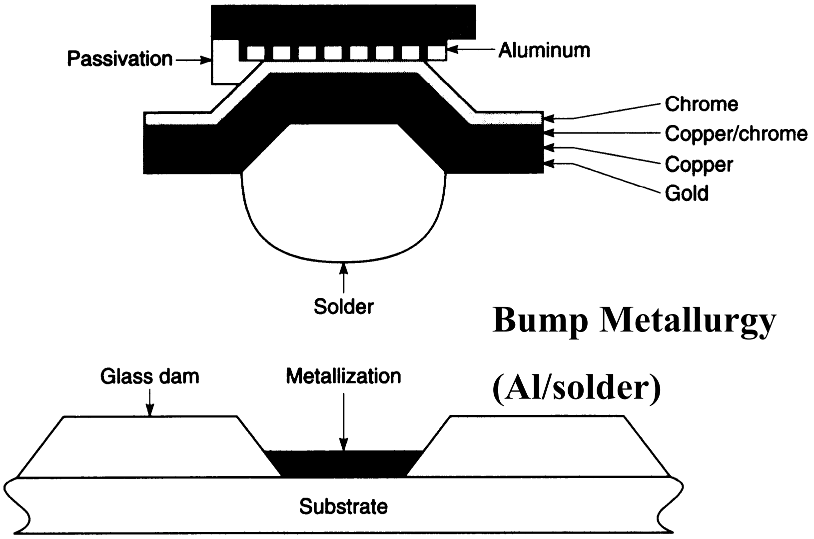

Bump Metallurgy (Al/solder)

Figure 2.18 Metallurgy of a solder bump used in flip chip bonding.

TABLE 2.12 Utilization and Properties of Materials Used in Flip Chip Bonding

Materials	Function
Cr, Ti, Pt, Al, Ti-W	Adhesion
Cu, Pd, W, Pt, Ni, Ti-W	Barrier
Au, Ti	Bonding
Au, Au-Cu, Solder-Cu	Bump
Cu	Leads
Sn, Au, Au–Ni	Plating on leads

		Bump Material	
Property	Gold	Copper	95Pb/5Sn
Tensile strength (MPa)	152–213	207–276	20
Elongation (%)	3.5–6.3	2–3	25
Young's modulus (GPa)	77	83	24
Resistivity ($\Omega \times 10^{-8}$)	2.0–2.5	1.75–2.0	20
Thermal cond. (W/m·K)	318	380	36
Temp. coef. exp. (ppm/°C)	15	17	29

Diffusion

Fick's first law

$$J = -D\,\partial c_x/\partial x$$

Fick's second law

$$\partial c_x/\partial t = \partial(D\,\partial c_x/\partial x)/\partial x \approx D\,\partial^2 c_x/\partial x^2$$

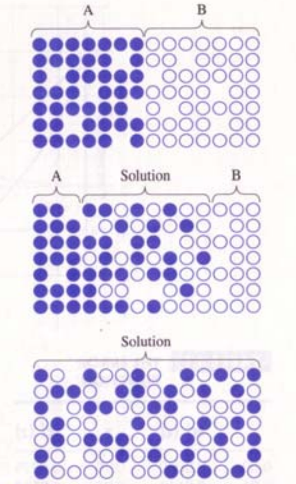

FIGURE 4-16 *The interdiffusion of materials A and B. Although any given A or B atom is equally likely to "walk" in any random direction (see Figure 4-15), the concentration gradients of the two materials can result in a net flow of A atoms into the B material, and vice versa. (From W. D. Kingery, H. K. Bowen, and D. R. Uhlmann, Introduction to Ceramics, 2nd ed., John Wiley & Sons, Inc., New York, 1976.)*

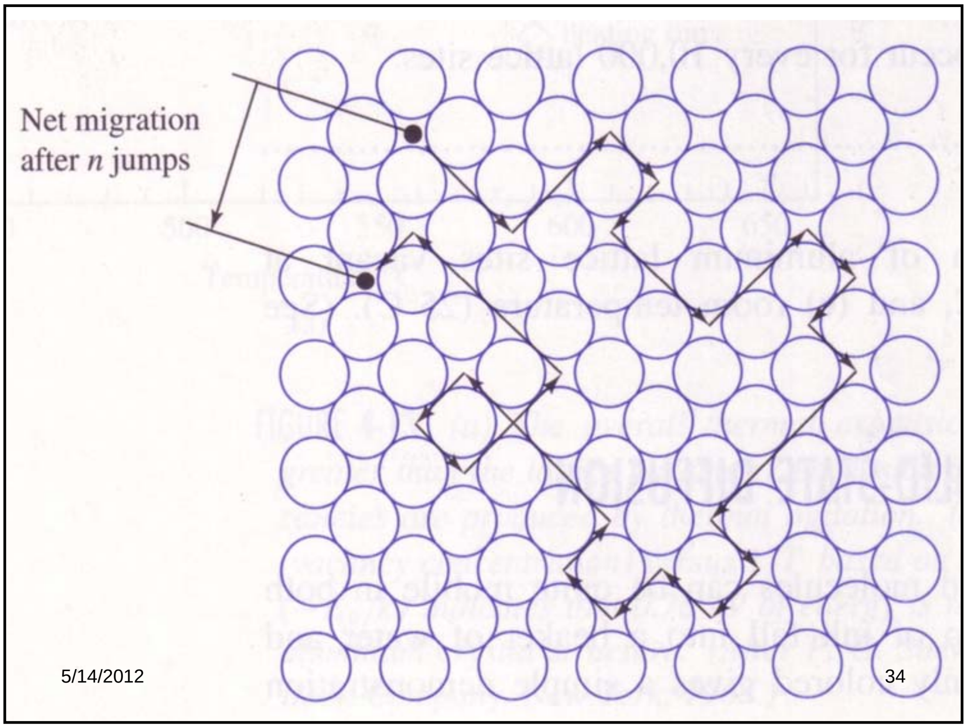

Solution (constant source):

$c_x = c_0 + (c_s - c_0)\ [1\text{-erf}\{x/2\sqrt{}Dt)]$

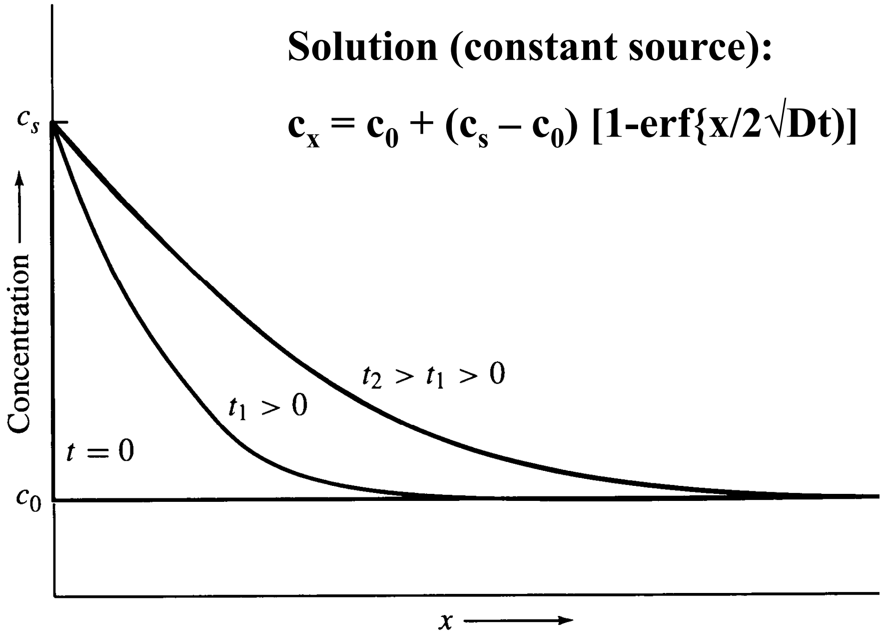

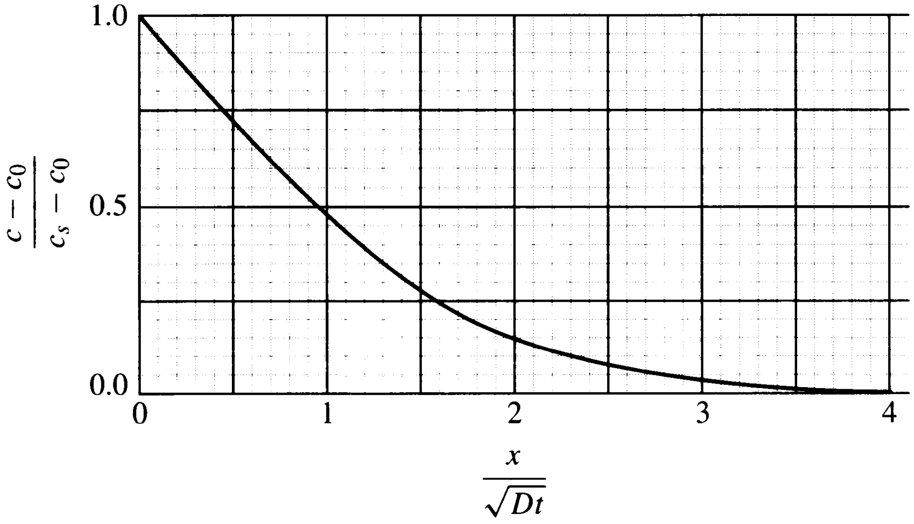

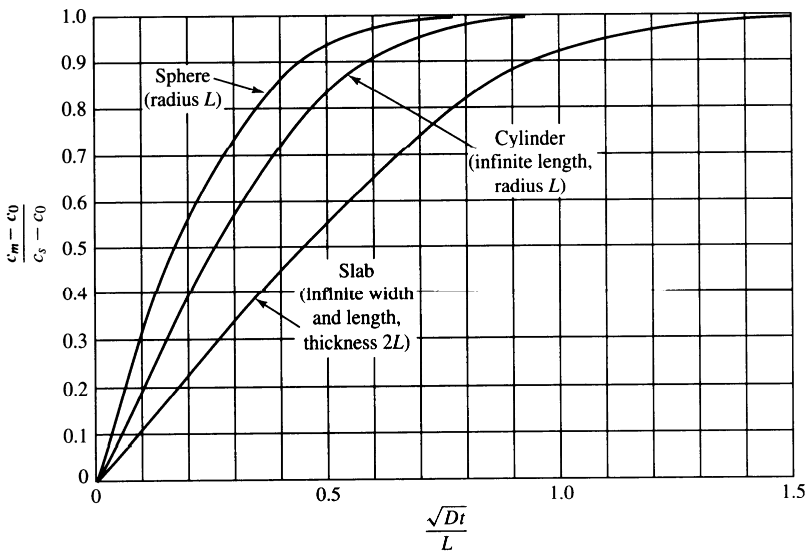

FIGURE 4-20 *Saturation curves similar to Figure 4-19 for various geometries. The parameter c_m is the average concentration of diffusing species within the sample. Again, the surface concentration c_s and diffusion coefficient D are assumed to be constant. (From W. D. Kingery, H. K. Bowen, and D. R. Uhlmann,* Introduction to Ceramics, *2nd ed., John Wiley & Sons, Inc., New York, 1976.)*

$D = D_0 \exp{-Q/kT}$

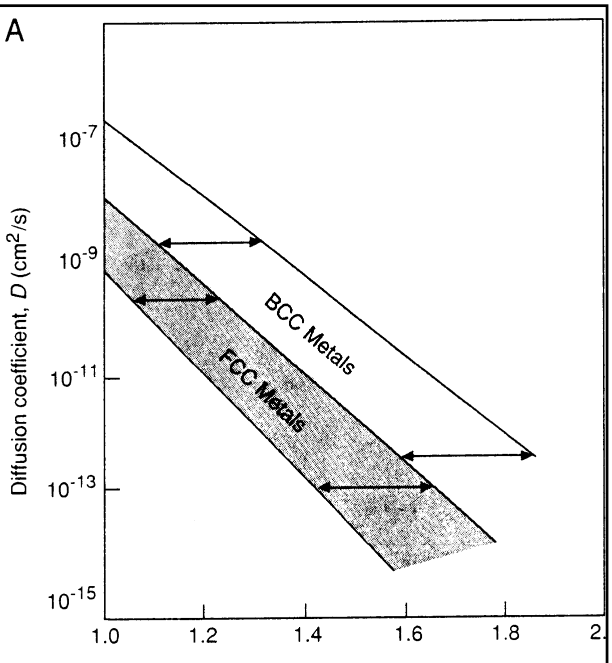

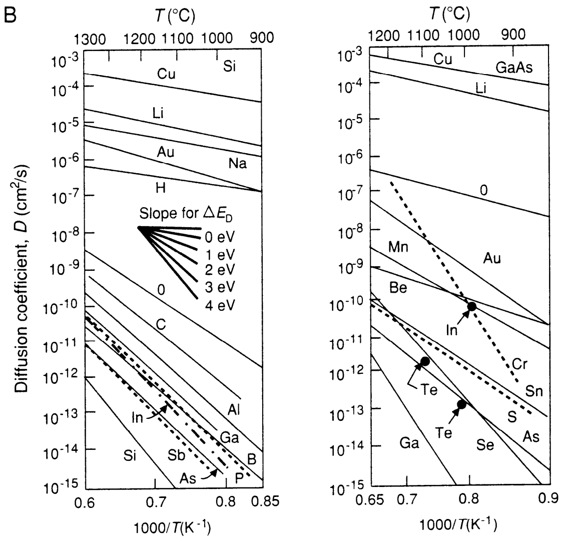

(A) Approximate range of diffusivity versus temperature for substitutional diffusion in BCC and FCC alloys. T_M is the melting point of the alloy. Adapted from O. D. Sherby and M. T. Simnad, *Transactions of the American Society for Metals* **54**, 227 (1961). (B) Diffusion of dopants in Si and GaAs. From S. M. Sze, *Semiconductor Devices: Physics and Technology*, Wiley (1985). Copyright © 1985 by AT&T; reprinted by permission. (C) Diffusion in oxide materials. *Note:* CSZ refers to stabilized ZrO_2. From W. Rhodes and R. E. Carter, *Journal of the American Ceramic Society* **49**, 244 (1966). Reprinted by permission of the American Ceramic Society.

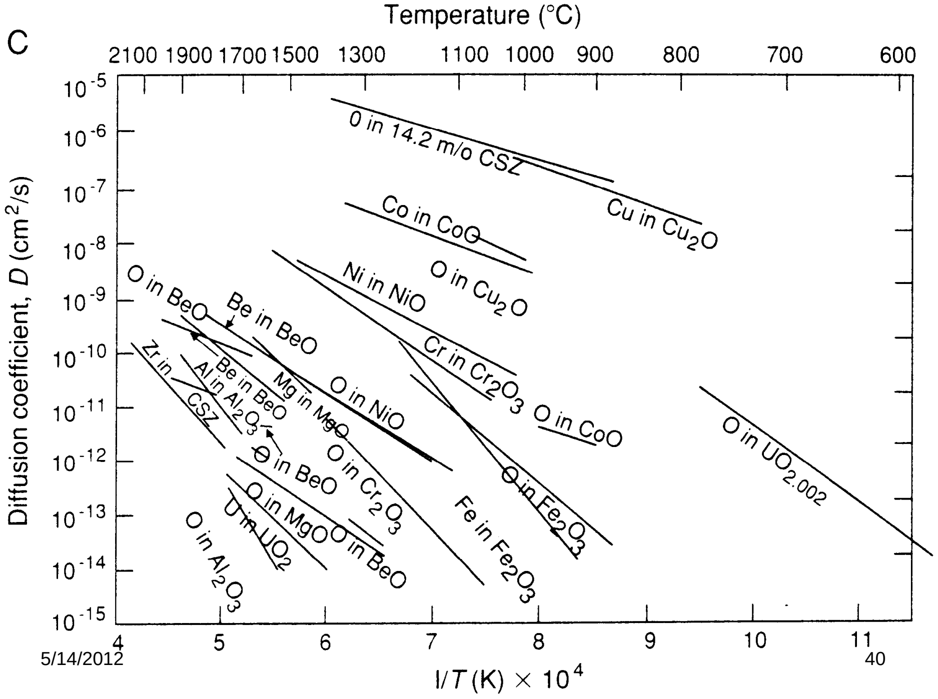

Note Cu in Al

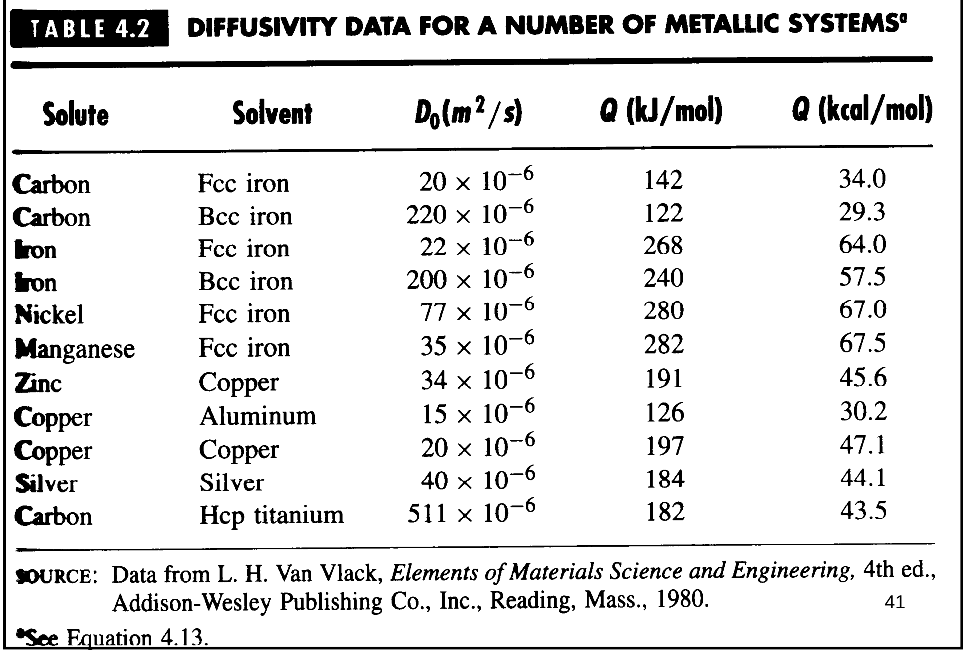

TABLE 4.2 **DIFFUSIVITY DATA FOR A NUMBER OF METALLIC SYSTEMS**[a]

Solute	Solvent	$D_0 (m^2/s)$	Q (kJ/mol)	Q (kcal/mol)
Carbon	Fcc iron	20×10^{-6}	142	34.0
Carbon	Bcc iron	220×10^{-6}	122	29.3
Iron	Fcc iron	22×10^{-6}	268	64.0
Iron	Bcc iron	200×10^{-6}	240	57.5
Nickel	Fcc iron	77×10^{-6}	280	67.0
Manganese	Fcc iron	35×10^{-6}	282	67.5
Zinc	Copper	34×10^{-6}	191	45.6
Copper	Aluminum	15×10^{-6}	126	30.2
Copper	Copper	20×10^{-6}	197	47.1
Silver	Silver	40×10^{-6}	184	44.1
Carbon	Hcp titanium	511×10^{-6}	182	43.5

SOURCE: Data from L. H. Van Vlack, *Elements of Materials Science and Engineering,* 4th ed., Addison-Wesley Publishing Co., Inc., Reading, Mass., 1980.

[a] See Equation 4.13.

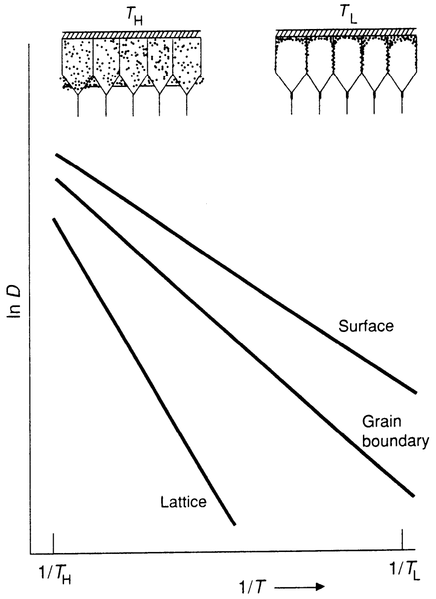

Schematic dependence of lattice, grain boundary, and surface diffusion on temperature. For operative lattice and grain boundary diffusion mechanisms, diffusional penetration is primarily through the bulk of the grains at high temperature (T_H). At low temperature (T_L), diffusional penetration of grain boundaries is dominant as shown in the above structural model.

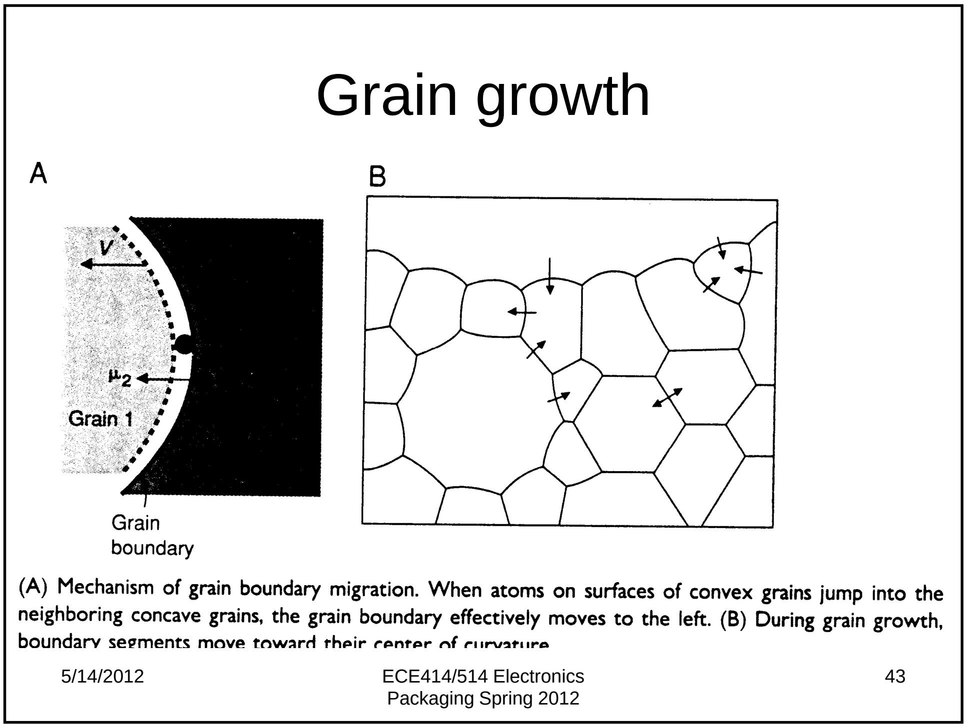

Grain growth

(A) Mechanism of grain boundary migration. When atoms on surfaces of convex grains jump into the neighboring concave grains, the grain boundary effectively moves to the left. (B) During grain growth, boundary segments move toward their center of curvature

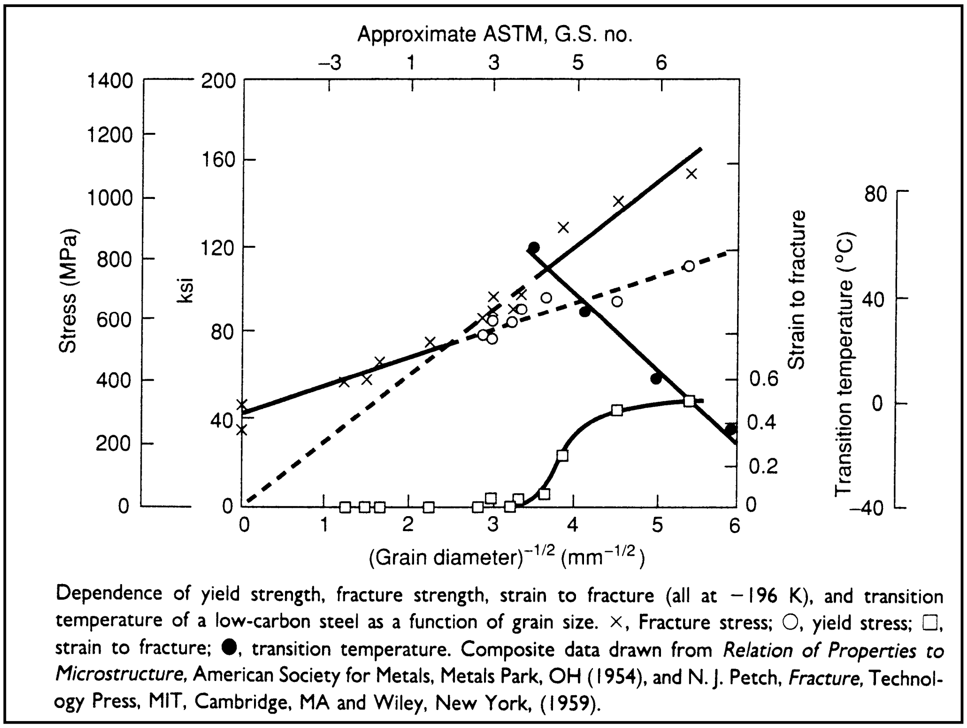

Dependence of yield strength, fracture strength, strain to fracture (all at − 196 K), and transition temperature of a low-carbon steel as a function of grain size. ×, Fracture stress; ○, yield stress; □, strain to fracture; ●, transition temperature. Composite data drawn from *Relation of Properties to Microstructure*, American Society for Metals, Metals Park, OH (1954), and N. J. Petch, *Fracture*, Technology Press, MIT, Cambridge, MA and Wiley, New York, (1959).

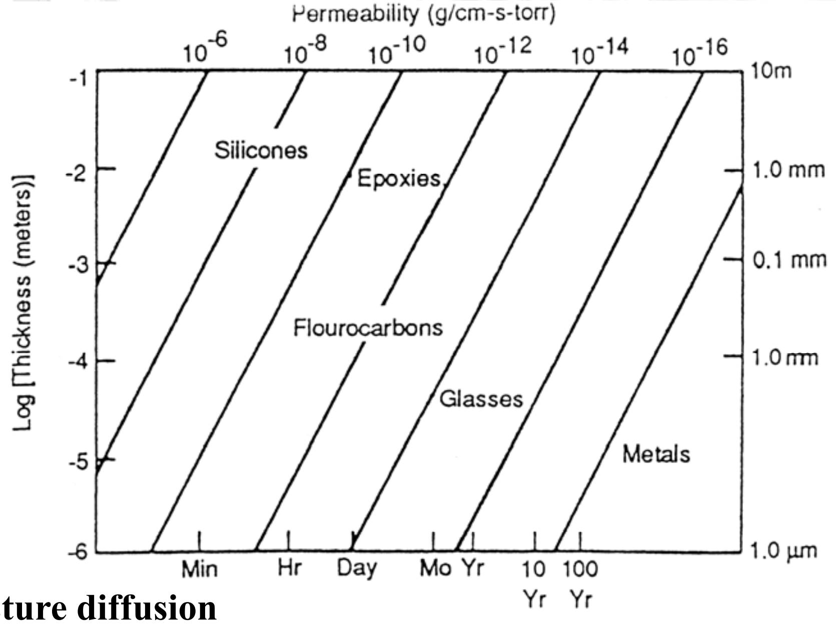

Moisture diffusion

Figure 10.3 Time for moisture to permeate various sealant materials in one defined geometry. (From Ref. 8.)

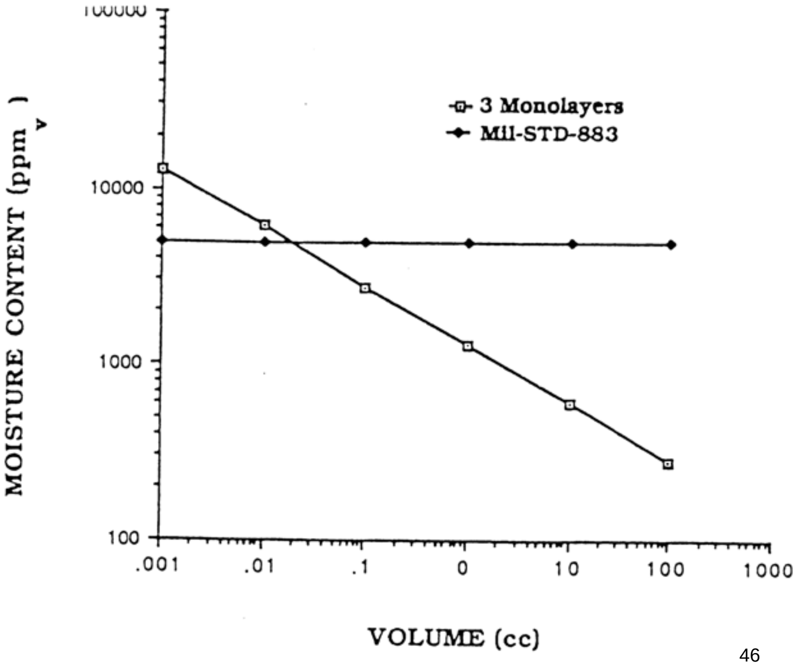

Figure 10.2 Amount of internal vapor that can result in three-monolayer coverage.

Die Attach

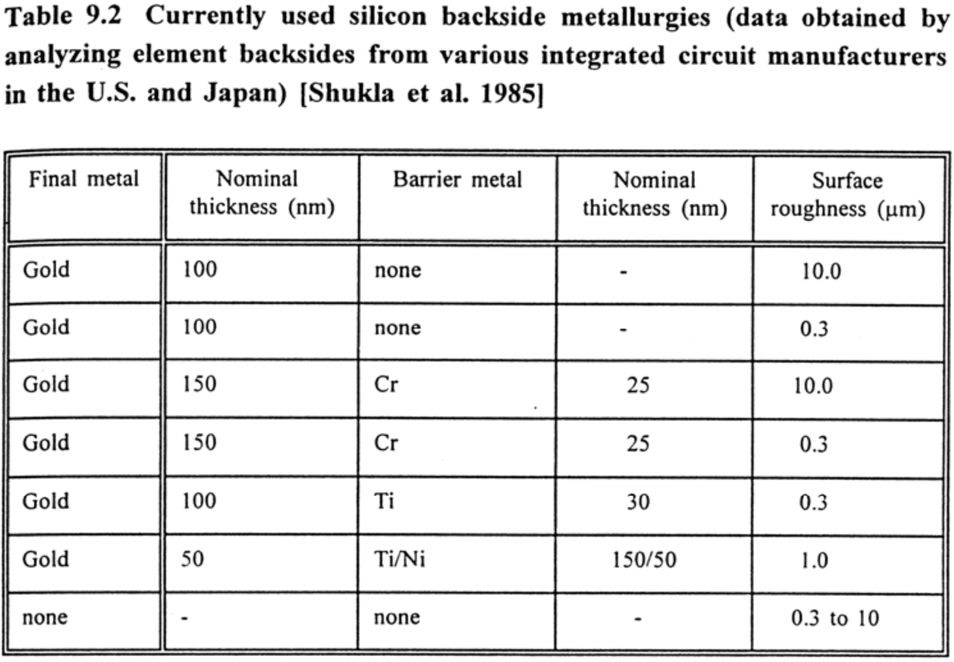

Table 9.2 Currently used silicon backside metallurgies (data obtained by analyzing element backsides from various integrated circuit manufacturers in the U.S. and Japan) [Shukla et al. 1985]

Final metal	Nominal thickness (nm)	Barrier metal	Nominal thickness (nm)	Surface roughness (μm)
Gold	100	none	-	10.0
Gold	100	none	-	0.3
Gold	150	Cr	25	10.0
Gold	150	Cr	25	0.3
Gold	100	Ti	30	0.3
Gold	50	Ti/Ni	150/50	1.0
none	-	none	-	0.3 to 10

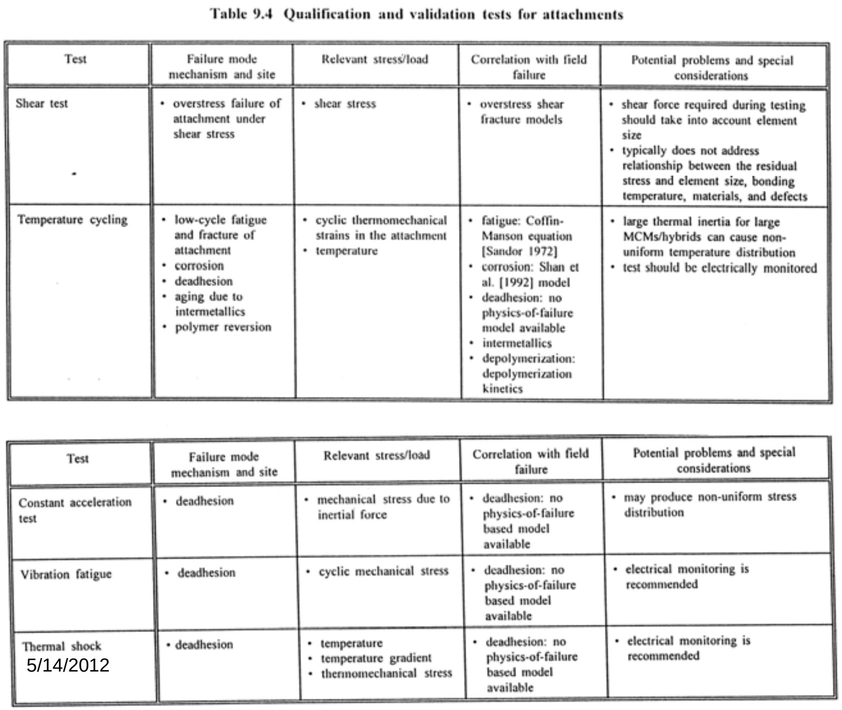

Table 9.4 Qualification and validation tests for attachments

Test	Failure mode mechanism and site	Relevant stress/load	Correlation with field failure	Potential problems and special considerations
Shear test	• overstress failure of attachment under shear stress	• shear stress	• overstress shear fracture models	• shear force required during testing should take into account element size • typically does not address relationship between the residual stress and element size, bonding temperature, materials, and defects
Temperature cycling	• low-cycle fatigue and fracture of attachment • corrosion • deadhesion • aging due to intermetallics • polymer reversion	• cyclic thermomechanical strains in the attachment • temperature	• fatigue: Coffin-Manson equation [Sandor 1972] • corrosion: Shan et al. [1992] model • deadhesion: no physics-of-failure model available • intermetallics • depolymerization: depolymerization kinetics	• large thermal inertia for large MCMs/hybrids can cause non-uniform temperature distribution • test should be electrically monitored
Constant acceleration test	• deadhesion	• mechanical stress due to inertial force	• deadhesion: no physics-of-failure based model available	• may produce non-uniform stress distribution
Vibration fatigue	• deadhesion	• cyclic mechanical stress	• deadhesion: no physics-of-failure based model available	• electrical monitoring is recommended
Thermal shock	• deadhesion	• temperature • temperature gradient • thermomechanical stress	• deadhesion: no physics-of-failure based model available	• electrical monitoring is recommended

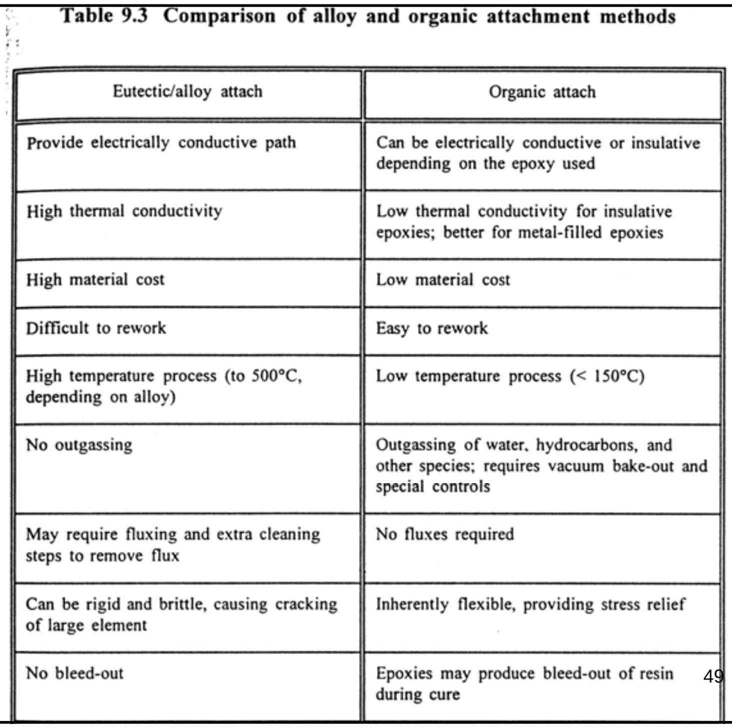

Table 9.3 Comparison of alloy and organic attachment methods

Eutectic/alloy attach	Organic attach
Provide electrically conductive path	Can be electrically conductive or insulative depending on the epoxy used
High thermal conductivity	Low thermal conductivity for insulative epoxies; better for metal-filled epoxies
High material cost	Low material cost
Difficult to rework	Easy to rework
High temperature process (to 500°C, depending on alloy)	Low temperature process (< 150°C)
No outgassing	Outgassing of water, hydrocarbons, and other species; requires vacuum bake-out and special controls
May require fluxing and extra cleaning steps to remove flux	No fluxes required
Can be rigid and brittle, causing cracking of large element	Inherently flexible, providing stress relief
No bleed-out	Epoxies may produce bleed-out of resin during cure

---

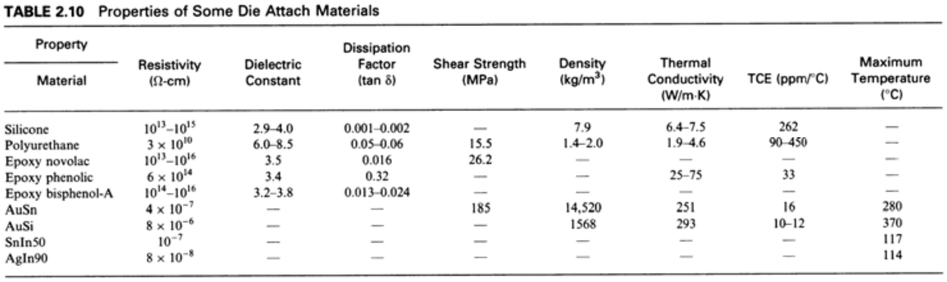

TABLE 2.10 Properties of Some Die Attach Materials

Property Material	Resistivity (Ω-cm)	Dielectric Constant	Dissipation Factor (tan δ)	Shear Strength (MPa)	Density (kg/m³)	Thermal Conductivity (W/m·K)	TCE (ppm/°C)	Maximum Temperature (°C)
Silicone	10^{13}–10^{15}	2.9–4.0	0.001–0.002	—	7.9	6.4–7.5	262	—
Polyurethane	3×10^{10}	6.0–8.5	0.05–0.06	15.5	1.4–2.0	1.9–4.6	90–450	—
Epoxy novolac	10^{13}–10^{16}	3.5	0.016	26.2	—	—	—	—
Epoxy phenolic	6×10^{14}	3.4	0.32	—	—	25–75	33	—
Epoxy bisphenol-A	10^{14}–10^{16}	3.2–3.8	0.013–0.024	—	—	—	—	—
AuSn	4×10^{-7}	—	—	185	14,520	251	16	280
AuSi	8×10^{-6}	—	—	—	1568	293	10–12	370
SnIn50	10^{-7}	—	—	—	—	—	—	117
AgIn90	8×10^{-8}	—	—	—	—	—	—	114

Ceramics

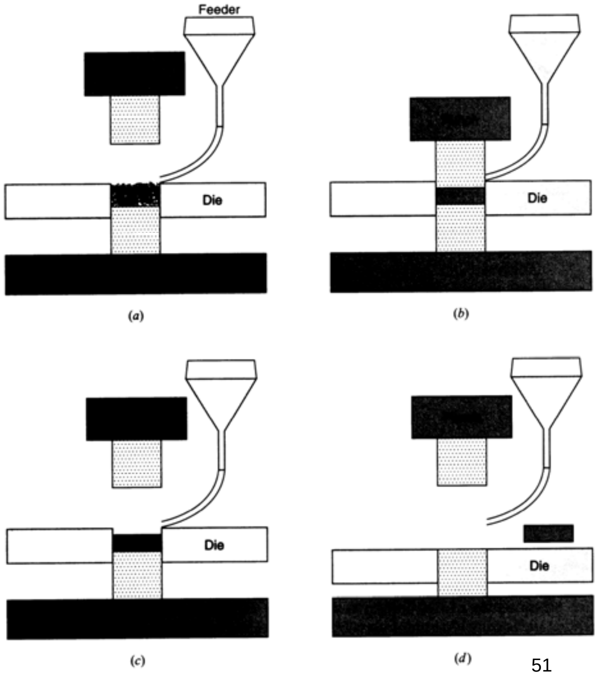

Figure 9.3 Dry pressing of ceramic substrates from powder.

LTCC

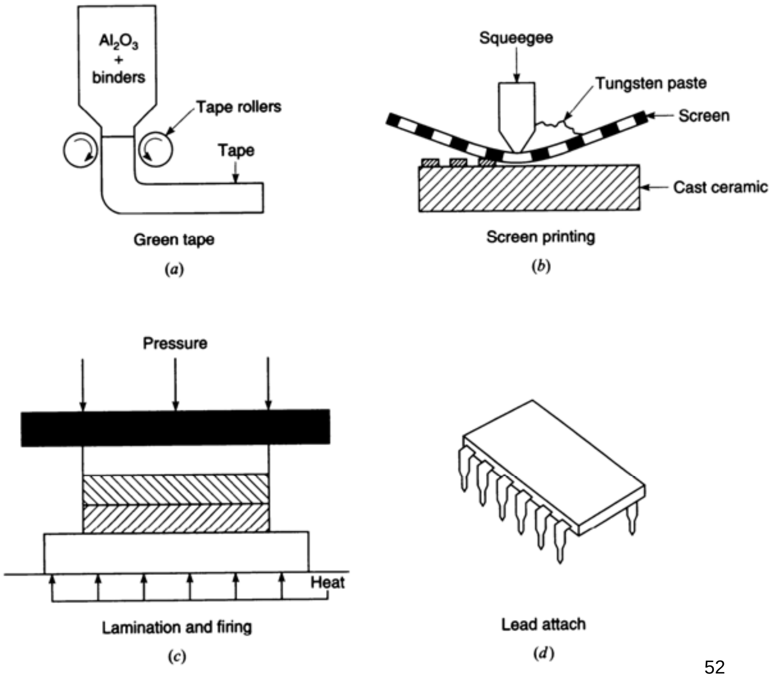

Figure 2.1 CERDIP — Laminated ceramic dual-in-line package.

Stencil/screen printing

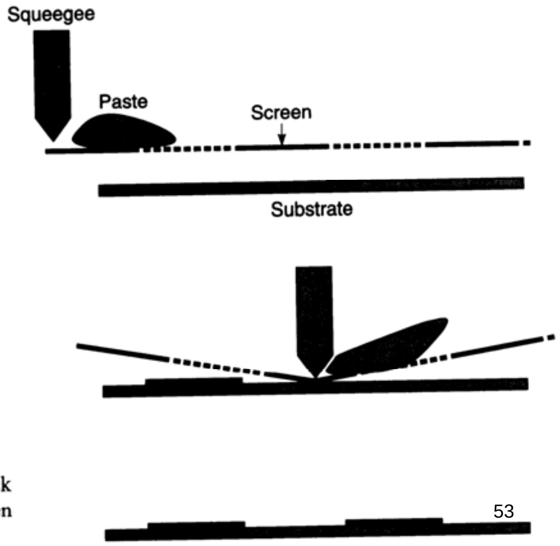

Figure 9.5 Schematic showing how thick film paste is dispensed in the screen printing process.

LTCC Processing

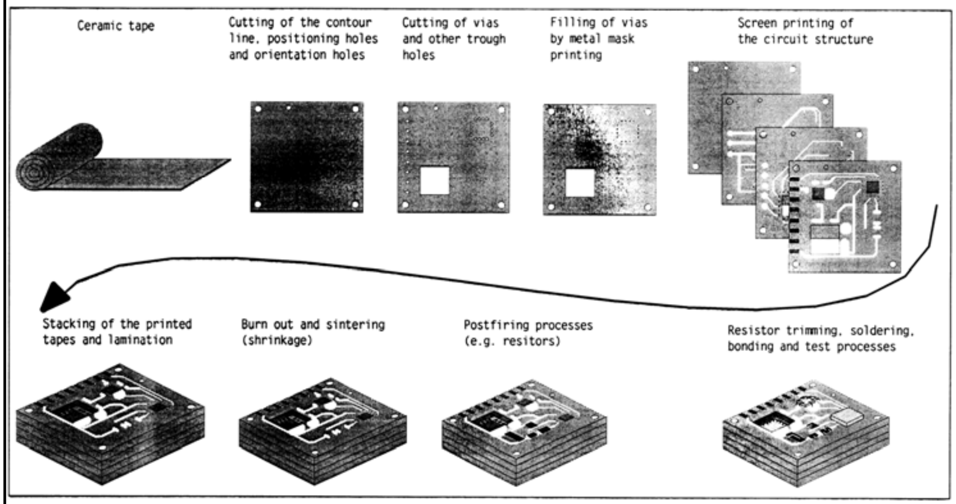

Fig. 1: Process steps of the Low Temperature Cofiring Multilayer Technology

3D LTCC packaging

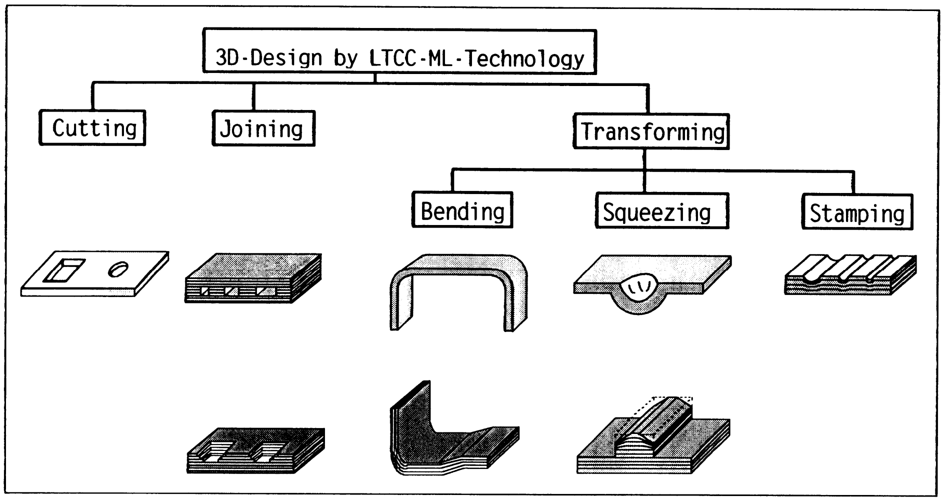

Fig. 2: Variants of possible three dimensional ceramic circuits

Ceramic materials properties

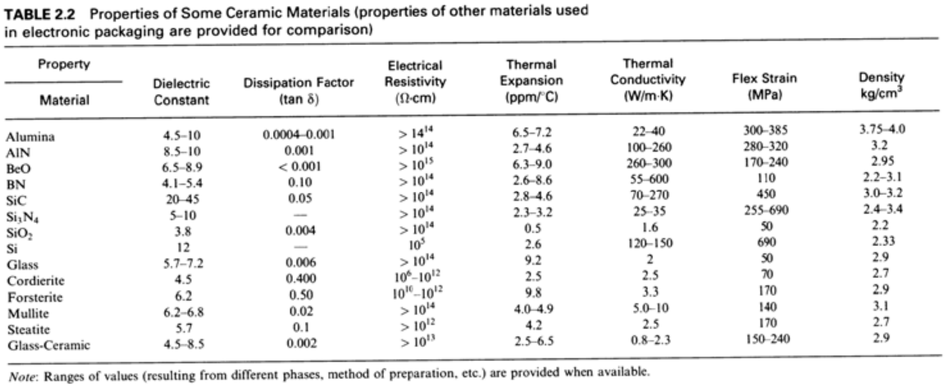

TABLE 2.2 Properties of Some Ceramic Materials (properties of other materials used in electronic packaging are provided for comparison)

Property Material	Dielectric Constant	Dissipation Factor (tan δ)	Electrical Resistivity (Ω-cm)	Thermal Expansion (ppm/°C)	Thermal Conductivity (W/m·K)	Flex Strain (MPa)	Density kg/cm^3
Alumina	4.5–10	0.0004–0.001	$> 14^{14}$	6.5–7.2	22–40	300–385	3.75–4.0
AlN	8.5–10	0.001	$> 10^{14}$	2.7–4.6	100–260	280–320	3.2
BeO	6.5–8.9	< 0.001	$> 10^{15}$	6.3–9.0	260–300	170–240	2.95
BN	4.1–5.4	0.10	$> 10^{14}$	2.6–8.6	55–600	110	2.2–3.1
SiC	20–45	0.05	$> 10^{14}$	2.8–4.6	70–270	450	3.0–3.2
Si_3N_4	5–10	—	$> 10^{14}$	2.3–3.2	25–35	255–690	2.4–3.4
SiO_2	3.8	0.004	$> 10^{14}$	0.5	1.6	50	2.2
Si	12	—	10^5	2.6	120–150	690	2.33
Glass	5.7–7.2	0.006	$> 10^{14}$	9.2	2	50	2.9
Cordierite	4.5	0.400	$10^6–10^{12}$	2.5	2.5	70	2.7
Forsterite	6.2	0.50	$10^{10}–10^{12}$	9.8	3.3	170	2.9
Mullite	6.2–6.8	0.02	$> 10^{14}$	4.0–4.9	5.0–10	140	3.1
Steatite	5.7	0.1	$> 10^{12}$	4.2	2.5	170	2.7
Glass-Ceramic	4.5–8.5	0.002	$> 10^{13}$	2.5–6.5	0.8–2.3	150–240	2.9

Note: Ranges of values (resulting from different phases, method of preparation, etc.) are provided when available.

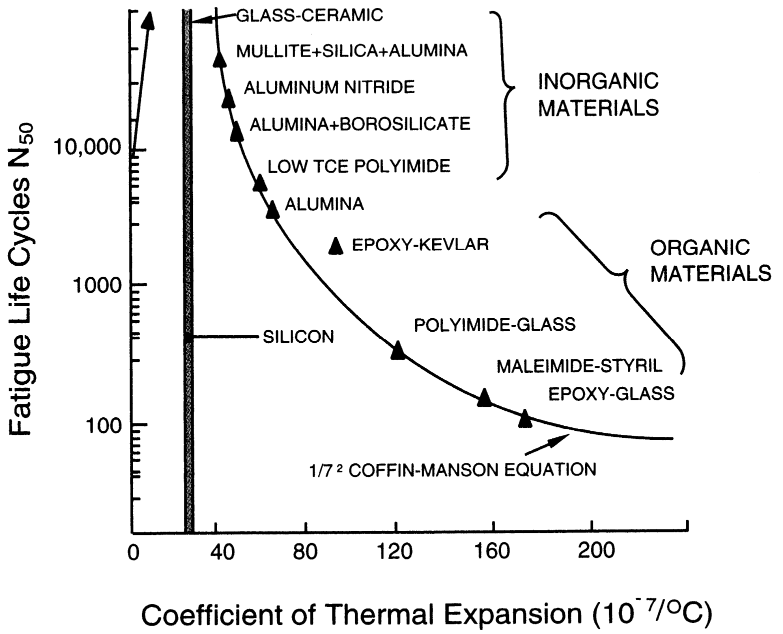

FIGURE 8.24 Fatigue life for MCM solder joints on various substrate materials versus the material's coefficient of thermal expansion.

Dielectric loss

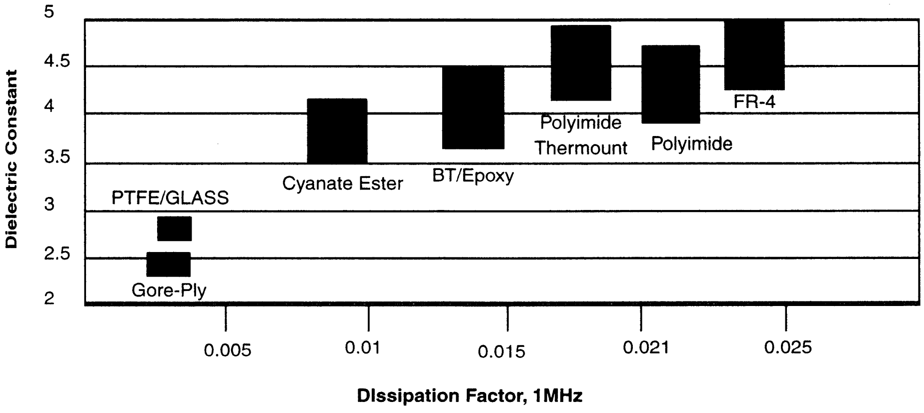

FIGURE 16.15 Electrical properties of various advanced PWB materials

FR4

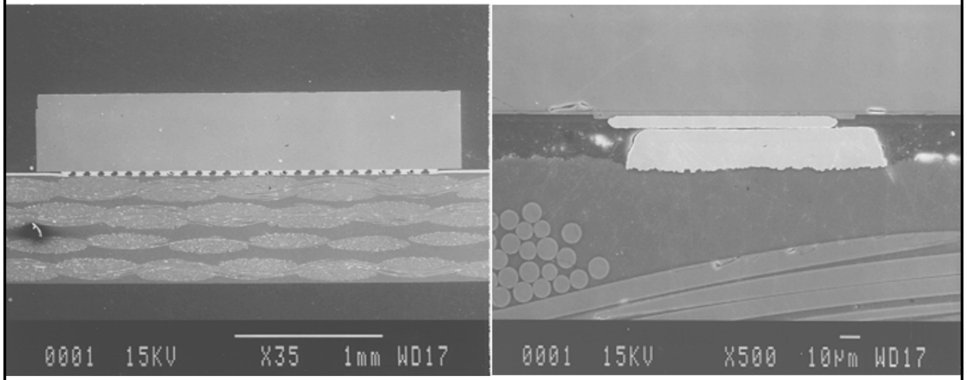

TABLE 2.14 Properties of Fiber Materials Used to Reinforce PCBs

Property / Material	Tensile Strength (kg/mm)	Elongation (Maximum) (%)	Thermal Conductivity (W/m·K)	CTE (ppm/°C)	Dielectric Constant (1 MHz)	Dissipation Factor (1 MHz)	Young's Modulus (kg/mm)
e-glass	350	4.9	0.9	5.0	5.9	0.0012	7500
s-glass	480	5.5	0.9	2.9	4.5	0.003	8500
Quartz	200	5.1	1.2	0.50	3.4	0.0002	7500
Aramid	410	4.5	0.5	60	4.05	0.001	12,800

FR4

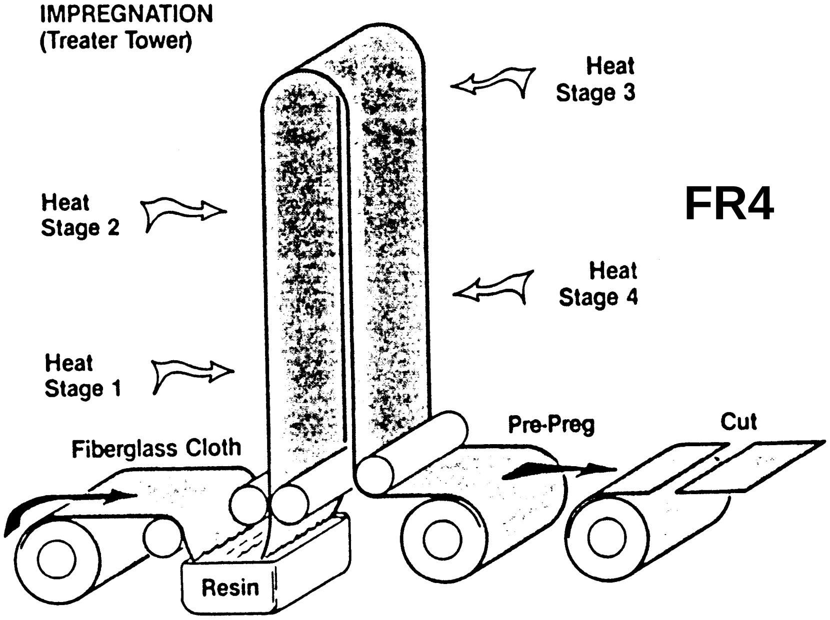

Figure 3. Describes the process which impregnates the woven glass cloth with resin.

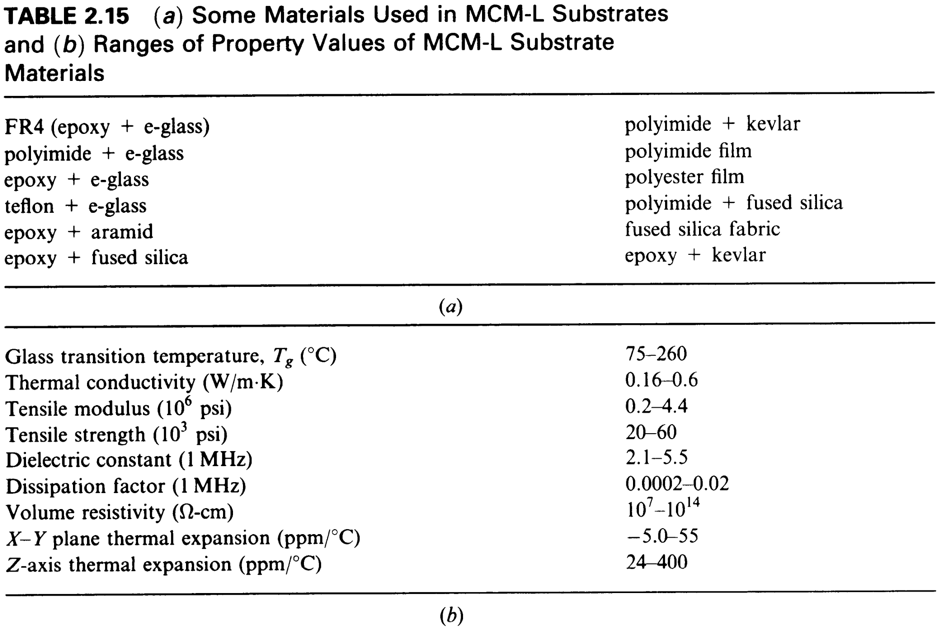

TABLE 2.15 (*a*) **Some Materials Used in MCM-L Substrates and** (*b*) **Ranges of Property Values of MCM-L Substrate Materials**

FR4 (epoxy + e-glass)
polyimide + e-glass
epoxy + e-glass
teflon + e-glass
epoxy + aramid
epoxy + fused silica
polyimide + kevlar
polyimide film
polyester film
polyimide + fused silica
fused silica fabric
epoxy + kevlar

(*a*)

Glass transition temperature, T_g (°C)	75–260
Thermal conductivity (W/m·K)	0.16–0.6
Tensile modulus (10^6 psi)	0.2–4.4
Tensile strength (10^3 psi)	20–60
Dielectric constant (1 MHz)	2.1–5.5
Dissipation factor (1 MHz)	0.0002–0.02
Volume resistivity (Ω-cm)	10^7–10^{14}
X–Y plane thermal expansion (ppm/°C)	−5.0–55
Z-axis thermal expansion (ppm/°C)	24–400

(*b*)

Lead-free Solder

- See Dally 7.5.3
- Environmental issues, legislation
- Binary alloys SnAg
- Ternary alloys
- Sn-Ag-Cu (SAC)
- NEMI standard and others
- iNEMI 95.5Sn3.9Ag0.6Cu